行政院國家科學委員會專題研究計劃成果報告

水文對坡地災害因子潛勢影響分析—總計劃暨子計劃：
震動引起孔隙水壓上升導致坡地崩坍影響之研究(I)
The Effects of Pore fluids Ascend Abruptly and Sloping Slide on Seismic Phenomenon (I)

計劃類別：□個別型計劃　■整合型計劃

計劃編號：NSC 90-2625-Z-002-025

執行期間：90 年 8 月 1 日至 91 年 7 月 31 日

整合型計劃：計劃主持人：譚義績

共同主持人：陳主惠

處理方式：□可立即對外提供參考

■一年後可對外提供參考

□兩年後可對外提供參考

（必要時，本會得延展發表時限）

執行單位：國立台灣大學生物環境工程學系

中華民國九十一年十月二十三日

Abstract..... I

中文摘要 II

Chapter 1 Introduction 1

Chapter 2 Hypotheses.....5

Chapter 3 Mathematical Model 6

3.1 Governing Equation.....6
3.2 Constitutive Equation.....7
3.3 Laplace Transform Solution.....11
3.4 Pore Pressure Dissipation at the Interface.....13

Chapter 4 Applications and Discussions.....16

Chapter 5 Conclusion.....25

Acknowledgements.....26

References.....27

Abstract

This study develops a simplified visco-elastic model to describe the ground water level changes in wells of Cho-Shui River alluvial fan after the Chi-Chi earthquakes in Taiwan. Assuming the porous media is undrained in a confined aquifer during the co-seismic period, an analytical solution is derived from the momentum equation of the liquid phase. The model was used to analyze the data collected over a high dense network of hydrologic monitoring wells in Cho-Shui River alluvial fan after the earthquakes. The simulated ground water level changes agree with the observed data. The result also showed that the viscosity coefficient of the model is strongly correlated to the hydraulic conductivity of the aquifer. According to the hydrogeological profiles provided by Central Geological Survey from the drilled cores, the highest groundwater level changes were located at the interface between the gravels and the sands in the confined aquifer. The field observation and the simulation result suggest the importance of hydrogeological conditions on the ground water changes during the Chi-chi earthquakes.

Keywords Chi-Chi earthquake, Groundwater level changes in wells, Visco-elastic model, Porous media

摘要

本研究研發一套簡易黏彈力學來探討集集大地震後地下水位之變化。假設孔隙水在地震期間在受壓含水層之地下水運動不能將水排出地層之情況之下推導出液相之動量方程式。

本模式收集濁水溪沖積扇目前水利署所建置之密集觀測網之資料，在地震發生之後之水位變化與黏彈模式分析之結果十分接近，其結果更顯示黏性係數與水力傳導係數十分密切之相關性。

根據中央地質調查所岩心鑽探，地下水位在地震前後變化較大之區域多為礫石與細砂之交接面，根據現地資料與模式分析結果更顯示地震時地下水位之變化多寡與水文地質環境有密切關聯性。

關鍵詞：集集大地震，地下水位變化，黏彈模式，孔隙介質

CHAPTER 1. Introduction

Cho-Shui River's alluvial fan is located in the mid-western plan of Taiwan and it has a drainage area about 1700 km^2. There are four major west-vergent-thrust faults accompanying with anticlines near the eastern side of the fan (Figure 1). The Chou-Shui river flows from east to west through two anticlinal hills, Dulliu and Baqua hill [Lin et al., 2000, 2001], and is the main recharge area of the fan. A Groundwater Monitoring Network System (GMNS), of evenly distributing 70 hydrological stations, including 188 monitoring wells drilled from depth 24 to 306 m, has been established in the fan since 1992. Each well is screened at one depth, and the groundwater levels are recorded automatically every hour (Hsu, 1998).

The drilled cores of the Cho-Shui River alluvial fan showed that the alluvial fan consists of several layers of Holocene to Pleistocene sands and gravels that formed the three aquifers separated by marine mud. The rising and falling mean sea levels due to the global climate change late in the Quaternary period formed the layered structure of the alluvial fan. Towards the west, the gravel layers become thinner while the mud layers thicken. Massive gravels are underlain at the upper fan (Central Geological Survey, 1994, 1999).

Central Geological Survey of Taiwan (1994, 1999) constructed 12 hydrogeological profiles based on the drilled core samples and three aquifers have been identified. Each aquifer can be divided horizontally into a confined part, located on the mid-tail fan and an unconfined part located

on the upper fan. In the confined part, gravelly sediments are found on the mid and the tail fan and the arenaceous sediments are on the tail fan. A clear interface between the gravels and the sands is located in the mid fan (Figures 2(a), and 2(b)).

At 01:47' 12.6" a.m. September 21, 1999, a large earthquake, M_L = 7.3 (the Richter magnitude), occurred in the middle of Taiwan. The epicenter was located at 23.87° N and 120.75 ° E near the town of Chi-Chi (Figure 3), and about 10 km away from the Chou-shui River's alluvial fan (Ma et al., 1999; Yu et al., 2001). The earthquake was caused by the motion of the Chelungpu thrust fault, adjacent to the west of the town of Chi-Chi. Another earthquake of a magnitude M_L = 6.9 occurred at 19:52'50.0" September 26, 1999 and the epicenter was located at 23.86° N and 121.00° E. The GMNS recorded the groundwater level fluctuations, ranging from 1 m to 7 m for the ascended levels and from -2 m to –11 m for the declined levels before and after these two earthquakes (Water Conservancy Agency, 1999a).

Rupturing of the Chelungpu fault in the Chi-Chi earthquake led to several meters of oblique thrust of the hanging wall. The GPS measurements (Department of Land Administration, 2000) showed only minor subsidence (< 0.5 m) in the Cho-Shui River alluvial fan after the two earthquakes [Department of Land Administration, 2000]. The ground water level fluctuations in well of the Cho-Shui river alluvial fan, however, showed changes up to a scale of an order greater than the subsidence right after the Chi-Chi earthquake (Water Conservancy Agency, 2000; Chia et

al., 2000). The distribution of ground water level changes monitored right after the first earthquake of September 21 is shown in Figure 3. The wells that recorded the negative water level changes in all depths were found close to the ruptured fault, and only in a narrow, belted area located between the Chelungpu thrust fault and the Changhwa thrust fault. This volumetric expansion zone in the footwall is possibly caused by dragging effects of the thrusting. Wells that recorded positive water level changes in all depths were mostly located away from the ruptured fault. The magnitude of the rise of the water level increases from the upper fan toward the mid fan and then decreases toward the tail fan. However, ground water levels in wells located right adjacent the western side of the Changwha thrust fault declined in one aquifer and ascended in all the other aquifers. The distribution of ground water level changes is not consistent with simulated strain fields (Huang, 2000). The inconsistency may be attributed to the fact that the ground water level changes were affected by heterogeneous sediments in the area neglected in strain models of the earthquake.

The objective of this study is to develop a model to describe the ground water level changes after the Chi-Chi earthquakes. A simplified visco-elastic model is constructed based on the hydrogeological condition of the area and an analytical solution of the model was derived. The solution was then applied to the groundwater level changes after the two earthquakes in the fan. Results of the analysis were used to explain the variation of ground water level observed in the GMNS.

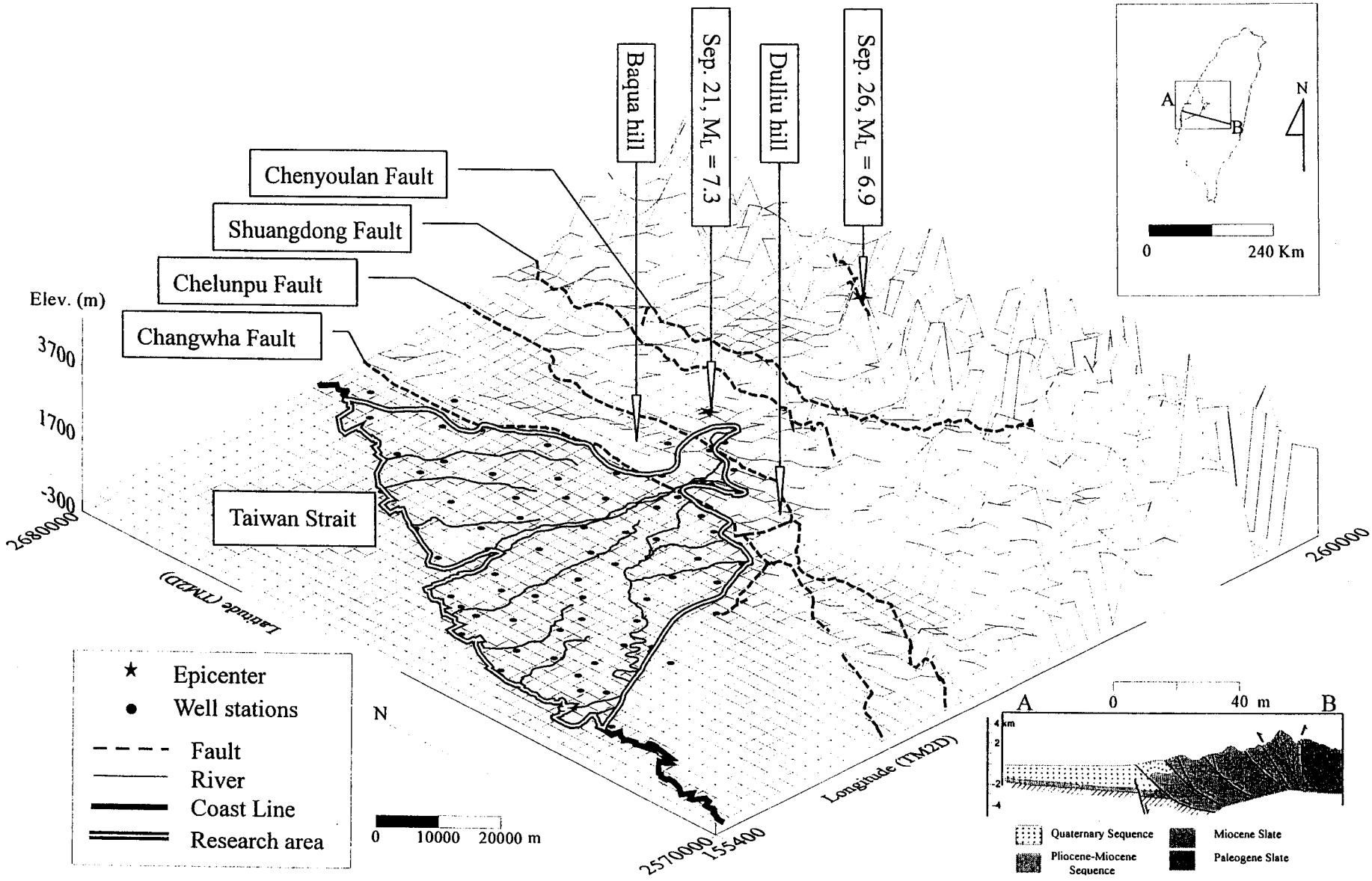

Figure 1. The geology and geography of the research are

CHAPTER 2. Hypotheses

According to the hydrogeological profiles provided by the Central Geological Survey [1994, 1999], the thickness of the aquifer decreases from the east to the west. Considering conservation of energy, when the wave caused by the earthquakes propagates from the east to the west, the change of the velocity of the wave will be significant towards the pinch-out of the aquifer. The influences of the inertial force on the ground water level fluctuations will increase toward the pinch-out. Therefore, we hypothesized that after the earthquakes the inertial force must be considered in a model for wave movement on the western side of the interface between the sands and the gravels. On the other hand, we believe the fluid behavior on the eastern side of the interface between the sands and the gravels obeys a diffusion equation.

CHAPTER 3. Mathematical Model

3.1 Governing Equation

Considering that the mixture theorem (Green and Naghdi, 1965) using the concept of pore pressure and the effective skeleton stress, the wave equation of the liquid phase can be described as (after Biot's notation) (Biot, 1956a, 1956b)

$$-\nabla\cdot\left(\varepsilon_f\nabla p^f\right)=\frac{\partial^2}{\partial t^2}\left(\rho_{sf}e+\rho_{ff}\varsigma\right)+b\frac{\partial}{\partial t}\left(\varsigma-e\right)+\upsilon^d\nabla\cdot b\,, \qquad (1)$$

where ε_f $\{\mathrm{L^3/L^3}\}$ is the void fraction of the liquid phase; p^f $\{\mathrm{M/T^2L}\}$ is the pressure of the liquid phase; $\rho_{sf}+\rho_{ff}=\rho^f\varepsilon_f$ $\{\mathrm{M/L^3}\}$ is the product of the density of the liquid phase and the void fraction of the liquid phase, ρ_{ff} denotes the effective mass of the liquid phase moving in the solid phase, ρ_{sf} represents the mass coupling between the liquid and the solid phase; $e=\nabla\cdot u_k^s$ $\{\mathrm{L/L}\}$ is the strain of the solid phase, while u_k^s $\{\mathrm{L}\}$ is the displacement of the solid phase in k direction; $\varsigma=\nabla\cdot u_k^f$ $\{\mathrm{L/L}\}$ is the strain of the liquid phase, while u_k^f $\{\mathrm{L}\}$ is the displacement of the liquid phase in k direction; $b=\mu{\varepsilon_f}^2/\mathrm{k}$ in which μ $\{\mathrm{M/TL}\}$ is the dynamic viscosity, ε_f $\{\mathrm{L^3/L^3}\}$ is the porosity, and k $\{\mathrm{L^2}\}$ is the intrinsic permeability, and υ^d $\{\mathrm{L/T}\}$ is the velocity of the liquid phase relative to the solid phase.

If we assume that $\nabla\varepsilon_f$, $\frac{\partial^2}{\partial t^2}\left(-\rho_{sf}e+\rho_{sf}\varsigma\right)$ and $\upsilon^d\nabla\cdot b$ are smaller than the other terms in (1), they can be neglected during the co-seismic and the post-seismic motion period. In other words,

there is no significant difference of b and ε_f, not homogeneous but with less significant difference of the gradient than other term in the equation, everywhere in the aquifer based on Biot's assumption (Biot, 1956a, 1956b). Because of the omission of the relative acceleration term, $\frac{\partial^2}{\partial t^2}\left(-\rho_{sf} e + \rho_{sf} \varsigma\right)$, (2) can only describe the quasi-static behavior of the liquid phase and is valid for the dissipation of the pore pressure after an earthquake. Moreover, the term, $b\frac{\partial}{\partial t}(\varsigma - e)$, is temporarily neglected. It will be reapplied when considering the constitutive equation, in which the viscosity coefficient is adapted to describe the pore pressure dissipation due to the relative velocity of the liquid phase and the solid phase. Then (1) can be rearranged as

$$\nabla^2\left(-\varepsilon_f p^f\right) = \frac{\partial^2}{\partial t^2}\left(\left(\rho_{sf} + \rho_{ff}\right)\varsigma\right) = \rho^f \frac{\partial^2}{\partial t^2}\left(\varepsilon_f \varsigma\right) \cong \rho^f \frac{\partial^2}{\partial t^2}\left(\nabla \cdot \left(\varepsilon_f u^f\right)\right). \qquad (2)$$

The number of the variables then is reduced from 3 (i.e., ς 、e 、p_f) in (1) to 2 (i.e., ς 、p_f) in (2). If no outflow of the fluid from the confined aquifer takes place during the co-seismic motion period, (2) is sufficient for the simulation of liquid phase behavior.

3.2 Constitutive Equation

In addition to (2), an equation is needed to find the exact solutions of the two variables. Considering the constitutive equation, an element such as a damping device can be adapted to represent the behavior of the liquid phase during the co-seismic period. If the liquid phase obeys the Maxwell-Fluid model (Figure 2(c)), the relation between stress and strain is

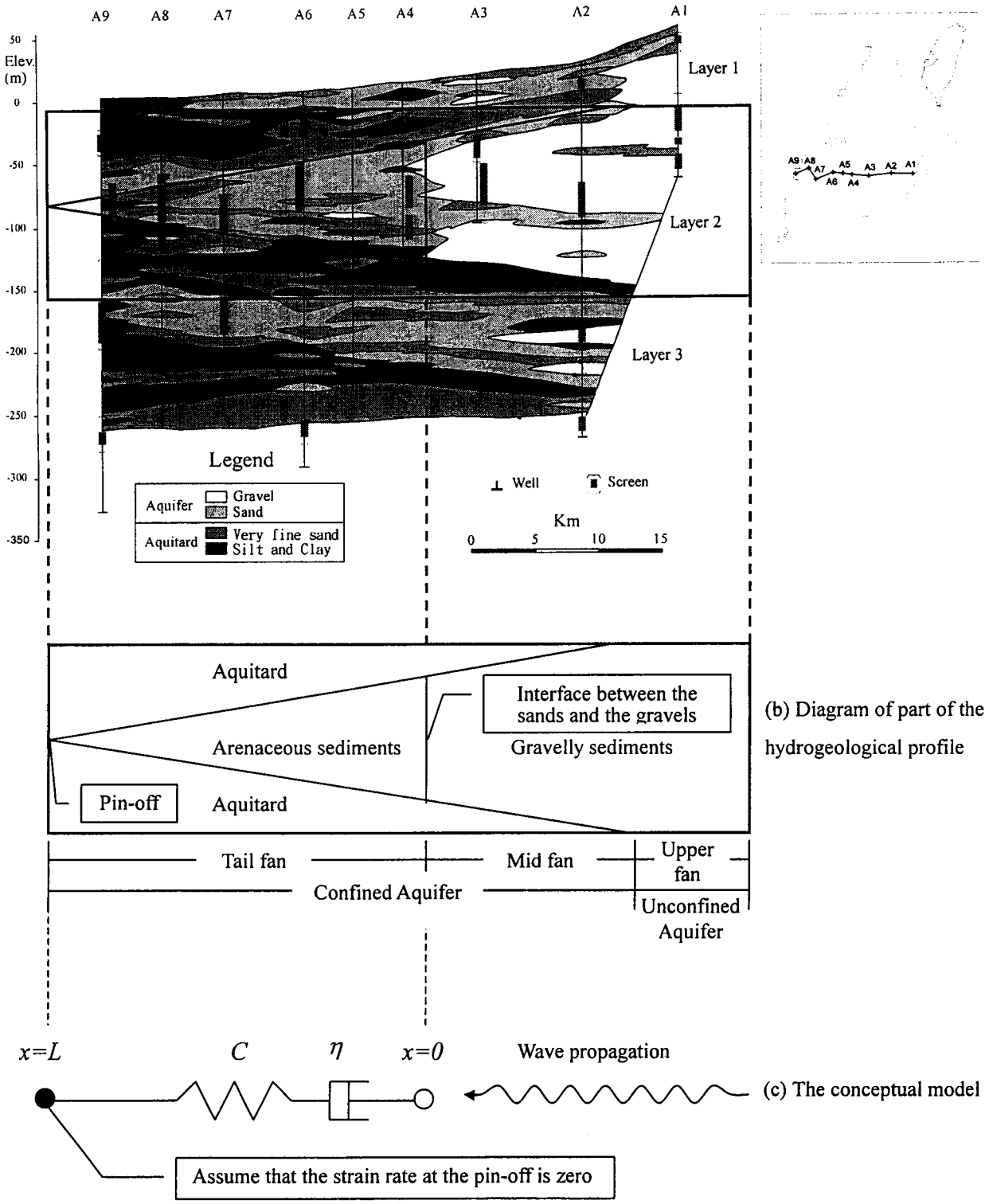

(b) Diagram of part of the hydrogeological profile

(c) The conceptual model

Figure 2. Conceptual model development

$$\left(-\varepsilon_f p^f\right)+\frac{\eta}{C}\frac{\partial}{\partial t}\left(-\varepsilon_f p^f\right)=\eta\frac{\partial}{\partial t}\left(\nabla\cdot\left(\varepsilon_f u^f\right)\right), \tag{3}$$

where C $\{\mathrm{M/T^2L}\}$ is the bulk modulus of the liquid phase, and η $\{\mathrm{M/TL}\}$ is the viscosity coefficient (i.e., the ratio of the pressure and the strain rate). The viscosity coefficient is utilized herein to describe the pore pressure dissipation that is caused by the relative velocity of the liquid phase and the solid phase. The advantage of such a substitution is that we need not to know the exact motion of the solid phase prior but only parameterize the equation to fit the observed records.

The rupture of the Chelunpu fault during the Chi-Chi earthquakes is parallel to the contour lines of the groundwater levels. Therefore, the 85-km rupture zone formed during the Chi-Chi earthquake is considered to supply a western-eastern direction aligned pressure simultaneously and uniformly to the fan (Figure 1 and 3). Based on this conjecture and for mathematical simplicity, we assumed a one-dimensional model is sufficient for the analysis of wave propagation in the area.

Considering one-dimensional flow, the horizontal displacement of the liquid phase per unit volume of the porous media is expressed as $\varepsilon_f u^f = e^{-\gamma x}e^{i(lx-wt)}$, where γ $\{\mathrm{1/L}\}$ is the attenuation coefficient; $i=\sqrt{-1}$; l $\{\mathrm{1/L}\}$ is the wave vector; and w $\{\mathrm{1/T}\}$ is the vibration frequency. The relationship between the strain rate of the liquid phase per unit porous media and the stress of the liquid phase per unit porous media can be described as

$$-\varepsilon_f p^f = \left(\frac{\eta}{1-\frac{w\eta i}{C}}\right)\frac{\partial\nabla\cdot\left(\varepsilon_f u^f\right)}{\partial t}. \tag{4}$$

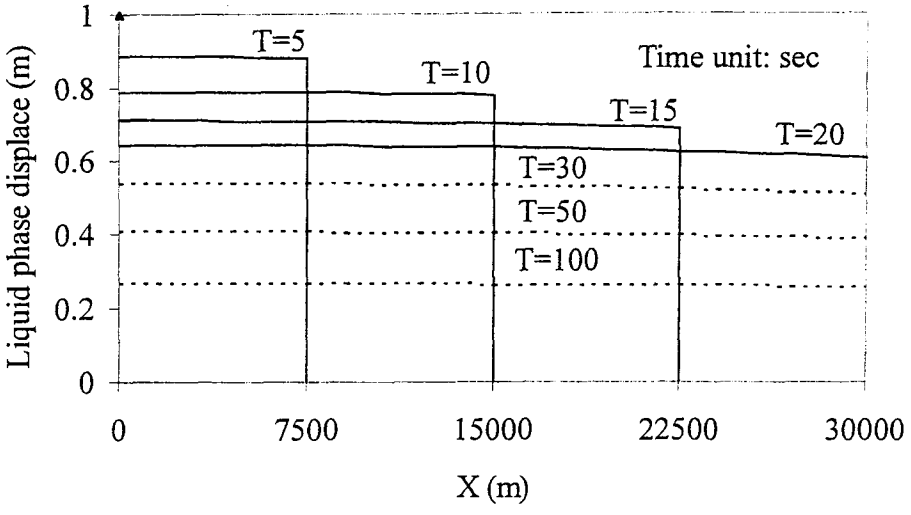

Figure 3. The time variable displacement, that is derived from the inverse Laplace transformation of equation (7), of the liquid phase at the arenaceous sediment void in the confined aquifer, and assume L=30000 m, v_f=1500 m/sec, η/C=20 day and $\frac{Fv_f}{C}$=1 m.

Upon combing with (4) and (2), and setting $U^f = \varepsilon_f u^f$, we have

$$\frac{\partial^2 U^f}{\partial x^2} - \frac{\rho^f}{\eta}\frac{\partial U^f}{\partial t} - \frac{1}{v_f^{\,2}}\frac{\partial^2 U^f}{\partial t^2} = 0, \tag{5}$$

where $v_f = \sqrt{C/\rho^f}$ { L/T } is the velocity of the wave propagation in the liquid phase.

3.3 Laplace Transform Solution

To analyze motion of the fluid phase in the confined aquifer of the alluvial fan, the boundary conditions of the conceptual model are set to be zero strain rate at x=L, and an impulse pressure at x=0 (see Figure 2(c)).

The initial condition of (5) is

$$U^f(x,0) = \frac{\partial U^f(x,0)}{\partial t} = 0 \tag{6}$$

With these boundary conditions and initial condition, we take the Laplace transform of (5) to project t into s and solve $U^f(x,t)$. Considering the constitutive equation, when the impulse pressure $P\delta(t)$ { M/T^{2}L } (where $\delta(t)$ has a dimension of { 1/T }) is implied at $x = 0$ (Figure 2(c)) and $t = 0$, and the strain at $x = 0$, is $\partial U^f(0,t)/\partial x = P\delta(t)\left(\frac{\eta}{C} + t\right)\Big/\eta$.

We take the Laplace transform of both sides of the above equation to project t into, and obtain $\frac{\overline{\partial U^f}}{\partial x}(0,s) = P\frac{1}{C}$, and substitute this into the Laplace transform of (5). We obtained

$$\overline{U^f}(x,s) = -\frac{Pv_f}{C\sqrt{s\left(\frac{C}{\eta}+s\right)}}e^{-\frac{x}{v_f}\sqrt{s\left(\frac{C}{\eta}+s\right)}}, \tag{7}$$

where $\overline{(\ )}$ represents the Laplace transform of variable $(\ )$.

Then the pore pressure per unit volume of the porous media was derived by taking the inverse Laplace transform (Farrell and Ross, 1971) of (7). The constant of the inverse Laplace transform was obtained by applying the boundary condition of zero strain rates, that is, $\frac{\partial}{\partial t}\left(\nabla \cdot U^f\left(L,t\right)\right)=0$. Therefore, considering (4), the pore pressure per unit volume of the porous media induced by unit pressure, $dp^f\left(x,t\right)$ {dimensionless}, can be expressed as (Flugge, 1995)

$$dp^f\left(x,t\right)=\delta t\frac{v_f}{C\varepsilon_f}\frac{\eta}{\sqrt{1+\frac{1}{Q^2}}}H\left(t-\frac{x}{v_f}\right)$$
$$\left\{\left[\frac{txI_1\left(\frac{C}{2\eta}\sqrt{\Delta}\right)e^{-\frac{C}{2\eta}t}}{2\frac{\eta}{C}v_f{}^2\Delta^{3/2}}+\frac{xI_1\left(\frac{C}{2\eta}\sqrt{\Delta}\right)e^{-\frac{C}{2\eta}t}}{4\left(\frac{\eta}{C}\right)^2 v_f{}^2\Delta^{1/2}}-\frac{tx\left[I_0\left(\frac{C}{2\eta}\sqrt{\Delta}\right)+I_2\left(\frac{C}{2\eta}\sqrt{\Delta}\right)\right]e^{-\frac{C}{2\eta}t}}{8\left(\frac{\eta}{C}\right)^2 v_f{}^2\Delta^{1/2}}\right]\right.$$
$$\left.-\left[\frac{tLI_1\left(\frac{C}{2\eta}\sqrt{\Delta_L}\right)e^{-\frac{C}{2\eta}t}}{2\frac{\eta}{C}v_f{}^2\Delta_L{}^{3/2}}+\frac{LI_1\left(\frac{C}{2\eta}\sqrt{\Delta_L}\right)e^{-\frac{C}{2\eta}t}}{4\left(\frac{\eta}{C}\right)^2 v_f{}^2\Delta_L{}^{1/2}}-\frac{tL\left[I_0\left(\frac{C}{2\eta}\sqrt{\Delta_L}\right)+I_2\left(\frac{C}{2\eta}\sqrt{\Delta_L}\right)\right]e^{-\frac{C}{2\eta}t}}{8\left(\frac{\eta}{C}\right)^2 v_f{}^2\Delta_L{}^{1/2}}\right]\right\} \tag{8}$$

where $\Delta=t^2-\left(\frac{x}{v_f}\right)^2$; $\Delta_L=t^2-\left(\frac{L}{v_f}\right)^2$; $H(\ )$ is the Heaviside function (O'Neil, 1991); δt is the total time of the co-seismic period; $I_n(\ )$ is the nth order Bessel function, where $I_n\left(x\right)=J_n\left(ix\right)$; and $Q=C/w\eta$. Notice that when $t<x/v_f$ the wave does not arrive at location x.

Hsieh et al. (1987) showed that the groundwater level changes in wells are less sensitive to the coefficient of storage than to the hydraulic conductivity. Based on (8), as the porosity increases or

η decreases, the pore pressure induced by earthquake decreases. Field data show the strong correlation between η and the hydraulic conductivity. This will be illustrated in the next section.

3.4 Pore Pressure Dissipation at the Interface

Consider that when the wave propagates from the unconfined aquifer to the confined aquifer through the interface between the gravels and the sands to the pinch-out and no leakage from one confined aquifer to another occurs during the co-seismic compression. Comparing the time scale of the model, daily average, with the dozens of seconds of the co-seismic period, the pressure induced by the earthquake could be simply regarded as an impulse pressure.

The decay of the impulse pressure at x=0 is described as follows. The force per unit length, F, of the earthquake leads to the sudden lift of the pore pressure at the interface between the gravels and the sands. Based on the Biot's derivation (Biot, 1941; Ge and Stover, 2000), if the force F $\{\mathrm{ML/T^2}\}$ is removed, the dissipation of the pore pressure, p_{bc}^{f}, obeys the diffusion equation and yields (Abramowitz and Stegun, 1972)

$$p_{bc}^{f}(x,t) = -\frac{e^{-\frac{x^2}{4\left(\frac{K}{S_s}\right)t}}}{2\varepsilon_f\sqrt{\pi t}}\frac{F}{\sqrt{\left(\frac{K}{S_s}\right)}}, \tag{9}$$

where S_s $\{\mathrm{1/L}\}$ is the specific storage of the aquifer; and K $\{\mathrm{L/T}\}$ is the hydraulic conductivity of the aquifer . When the impulse pressure is applied on the liquid phase, the displacement takes place simultaneously along the direction of the force. The energy is transmitted via the wave

propagation from the upper fan to the tail fan, and is dissipated due to the viscosity between the liquid phase and the solid grain. The energy is proportional to square of the displacement, so the displacement will decrease along with the time and the distance of the wave propagation (Figure 4). Because of the unbalance pressure head and the fluid characteristic, the liquid phase flows from high pressure to low pressure after the impulse pressure is removed. That is, it flows from the interface of the sands and the gravels to both sides upstream and downstream of the Cho-Shui River alluvial fan after the Chi-chi earthquake. Hence, the temporal variation of the pore pressure at the interface is $p_{bc}^{f}(0,t)=\frac{1}{2\varepsilon_f\sqrt{\pi t}}\frac{F}{\sqrt{\left(\frac{K}{S_s}\right)}}$. The pore pressure of the arenaceous sediments, p_{res}^{f}, therefore can be expressed in the convolution form of p_{bc}^{f} and dp^{f} as

$$p_{res}^{f}(x,t)=\int_0^t p_{bc}^{f}(0,t)\,dp^{f}(x,t-\tau)\mathrm{d}\tau . \qquad (10)$$

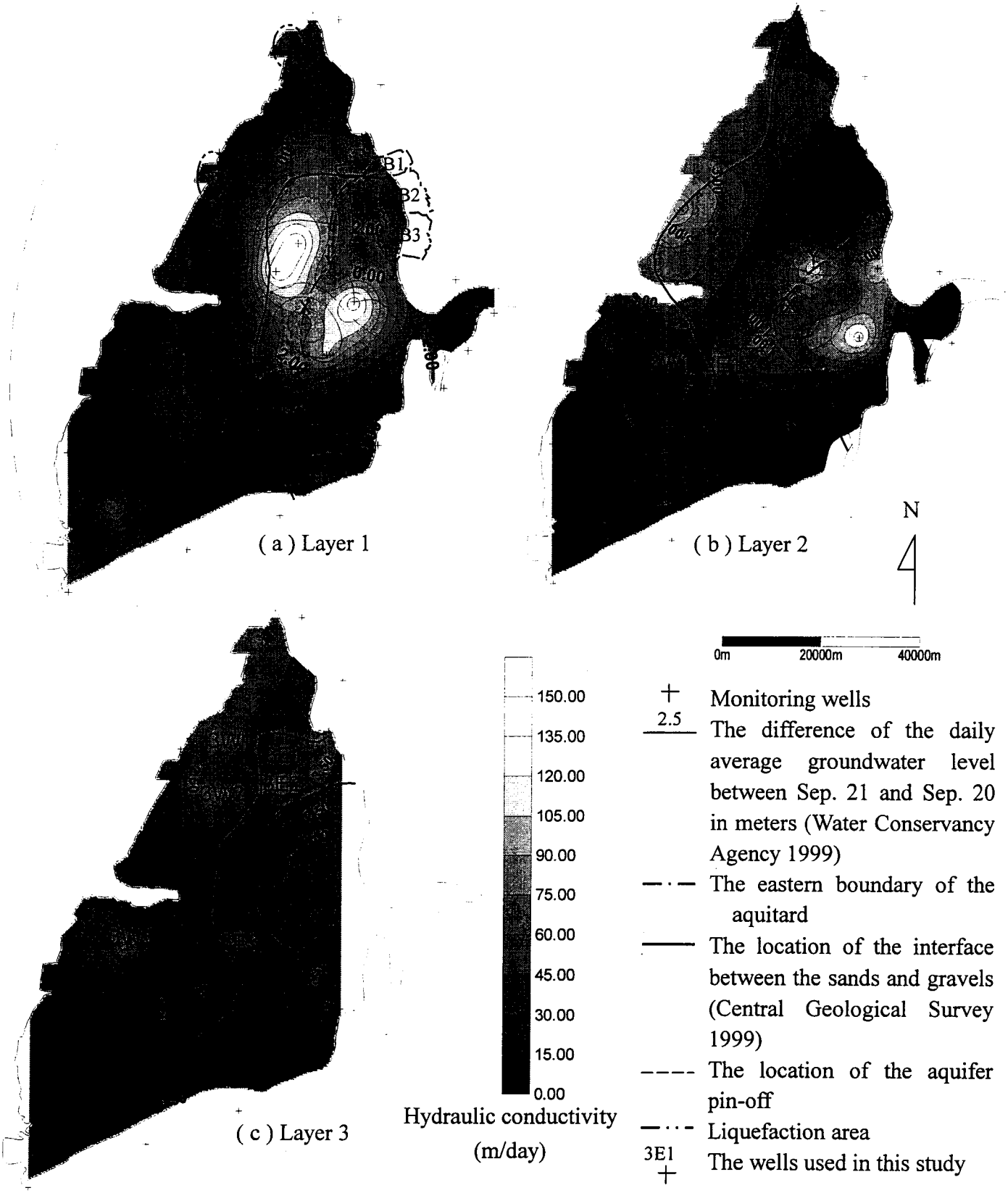

Figure 4. The relation of the distribution of the groundwater level changes in the wells and the hydrogeology

CHAPTER 4. Applications and Discussions

Four sets of wells, two wells in each set, were examined in the Cho-Shui River alluvial fan. Wells of the same set are chosen at the different side of the interface and the numbers assigned are in the form of, i.e. 3W1. The first number denotes the aquifer where well screened is located, i.e. 3 for aquifer 3. The second letter indicates the plane position of the well, i.e. W for west. The last number indicates the set number of the well, i.e. 1 for the first set of aquifer 3.

The pore pressure dissipation at the interface was determined by (9) using with the groundwater level records of the eastern well, L_{bc}, K and S_s (see Table 1). Values of parameters K and S_s were obtained from previous pumping tests (Water Conservancy Agency, 1999a) and L_{bc} is the horizontal and western-eastern direction aligned distance from the interface between the gravels and the sands to the wells located aside. Then the η value of the western well was found by fitting the simulated water level changes to the observed data with the consideration of the pore pressure dissipation previously obtained as the boundary condition of (10).

Two sets of wells were chosen--wells, 3E1, 3W1, 3E2 and 3W2 (Figure 5(c))--to verify the model. The records of the well 3E1 and the well 3E2 were substituted into (9) to obtain water level changes at the interface. Then the records of the well 3W1 and the well 3W2 were substituted into (10) to estimate the viscous coefficient. The results are shown in Figures 6 and 7 for Wells 3E1 and

Table 1. The fitting parameters of the wells used in this study

Well No. *	L_{hc} (m)	Position (TM2D, central meridian = 121°E)		Storage coefficient S **	Hydraulic conductivity k (m/day)**	The horizontal distance between the eastern well and the western well (m)	$\frac{\eta}{C}$ (day)
2E1	0	185350	2624184	0.00080	12.355	6682	0.19
2W1	6600	178717	2624989		30.499		
3E1	450	194052	2656100	0.00075	26.870	3934	0.64
3W1	3500	190120	2656250		56.572		
3E2	2000	196133	2649778	0.00114	52.445	8613	0.00025
3W2	6000	187624	2648441		67.133		
3E3	680	191168	2627781	0.00025	29.894	12746	7.2
3W3	12000	178717	2624989		11.568		

* Notation of the well number: The first number indicates the well screened at the assigned aquifer, i.e. 3 for aquifer 3. The second letter indicates the position of the well, i.e. W for west an E for east. The last number indicates the set number of the same aquifer, i.e. 1 for the first set.

**Data obtained by the well pumping tests. (Water Conservancy Agency 1999)

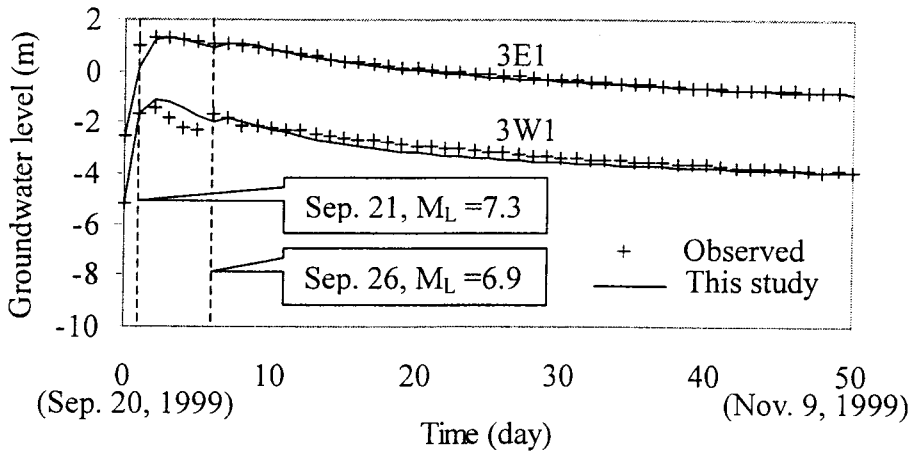

Figure 5. The comparison of observed and simulated groundwater level in the wells 3E1 and, 3W1

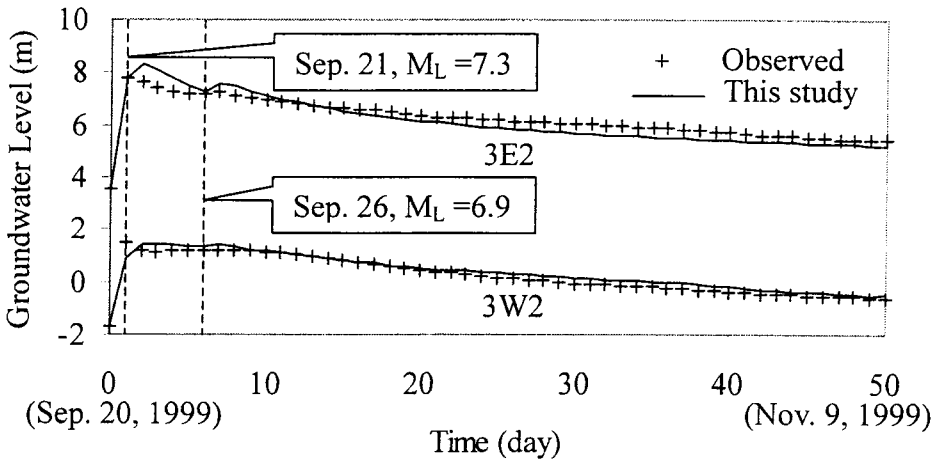

Figure 6. The comparison of observed and simulated groundwater level in the wells 3E2 and, 3W2

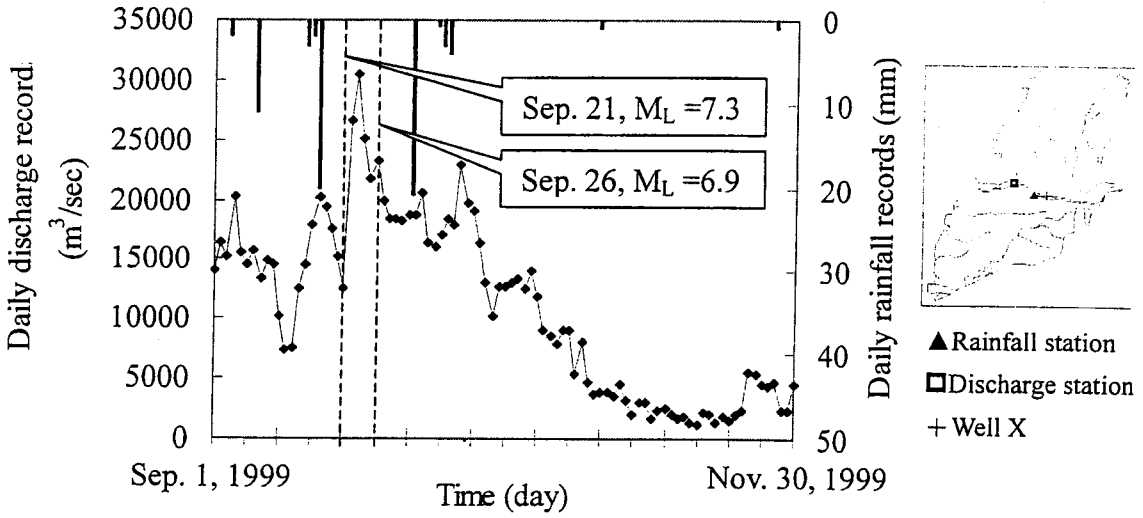

Figure 7. The suddenly arisen flow at the downstream Cho-Shui River beneath the well X. There is no rain after November 17, the arisen flow rather than the decayed flow was recorded right after the two earthquakes happened.

3W1, and Wells 3E2 and 3W2, respectively. In general, the simulated groundwater levels agree well with the observed, suggesting the quasi-static model is adequate to describe the ground water level changes.

Another two set of wells were also used as shown in Figure 5(b) and 5(c), assigned as 3E3, 3W3, 2E1 and 2W1, on the southern part of the fan for the analysis. The well 3W3 and the well 2W1 are located at the same position with different screen depths. The simulated results are plotted along with the observed data in Figure 9. The observed dissipation of the pore pressure in the well 2E1 is faster than simulated. This may be attributed to a multidimensional diffusion process and leakage between aquifer, which were neglected in the one-dimensional model. Based on the hydrogeological profiles constructed by the Central Geological Survey (1999), the position of 2E1 is located near the location X shown in Figure 4(a), which is a discharge area of the Cho-Shui River alluvial fan. A sudden increasing flow in the channel of the Cho-Shui River downstream the well X was observed (Figure 8) after the Chi-Chi earthquake (Water Conservancy Agency, 1999b). According to the Water Conservancy agency records [1999c], there was no rain after November 17. The sudden increase in flow may be attributed to groundwater discharge from aquifer 1. This appears to be caused by the increasing head in aquifer 2 and decreasing the head in aquifer 1, which induced the vertical water movement from aquifer 2 to aquifer 1. The vertical water movement may also occurred from aquifer 3 to aquifer 1. Although there is no aquitard between aquifer 2 and

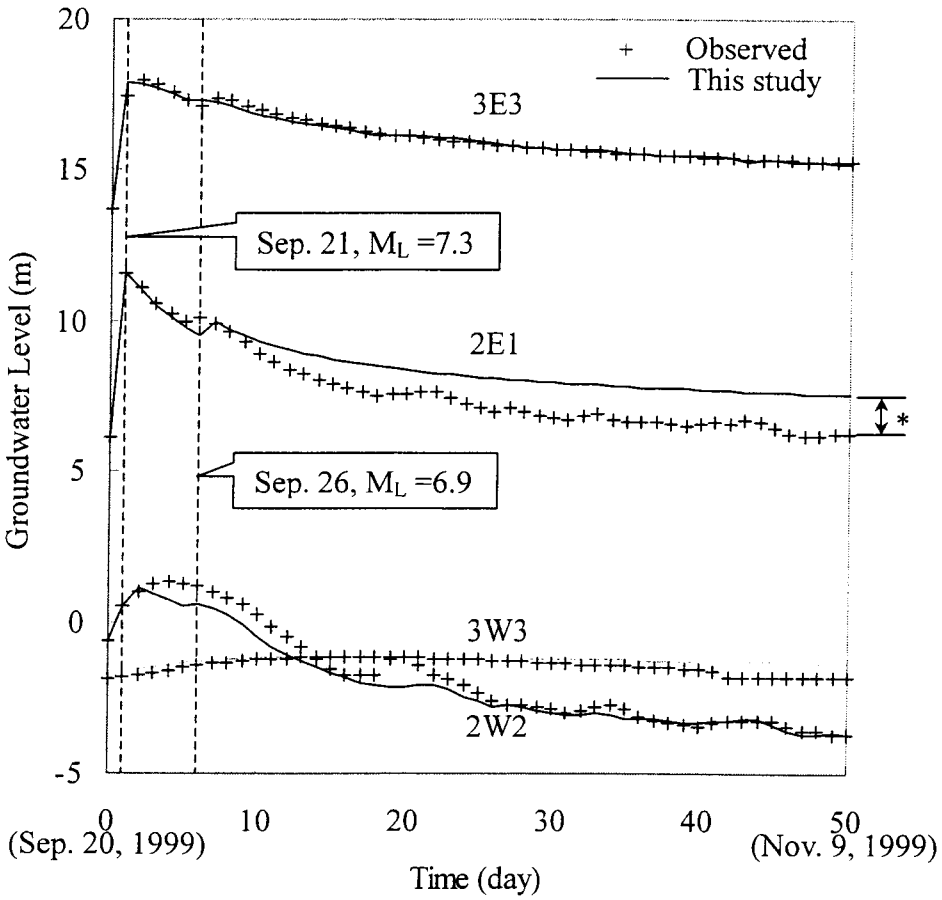

*The pore pressure dissipation doesn't obey the one dimension assumption in equation (9) due to the vertical flow in the unconfined aquifer, but it still can be substituted into equation (10) as the boundary condition.

Figure 8. The comparison of observed and simulated groundwater level in the wells 3E3, 3W3, 2E1 and 2W1

aquifer 1 to prevent a vertical water movement, an aquitard exists between aquifer 2 and aquifer 3 to retard the vertical flow nearby the position of the location X. This may explain the observation that the decrease of ground water level in the well 2E1 is faster than the simulated result while there is no significant difference between the observed and simulated diffusion of the well 3E1. Similar phenomena were found near the location Y. That is, the shape of the contour lines of the groundwater changes in the aquifer is similar to the shape of the eastern boundary of the aquitard as shown in Figure 5(b) and 5(c). The field observation suggested that the vertical water movement was significant in unconfined aquifer.

With the best-fit parameters, a regression between $Ln\left(\frac{\eta}{C}\right)$ and kL_{bc} was carried out and the result is shown in Figure 10. The relation can be expressed as

$$\frac{kL_{bc}}{1000} = -1.6401 Ln\left(\frac{\eta}{C}\right) + 2.943. \qquad (11)$$

The correlation coefficient is 0.9831. Equation (11) shows that the viscosity dissipation is proportional to the negative exponential of the distance. In general, the further the well is from the interface, the less the well is affected by the interface due to the viscosity dissipation. If the hydraulic conductivity increases, the relative displacement and the dissipation of the pore pressure occur easily, or η decreases. Substituting η obtained from equation (11) into equation (8) reveals that the increasing pore pressure and decreasing decay are at the boundary where hydraulic conductivity and the porosity decrease.

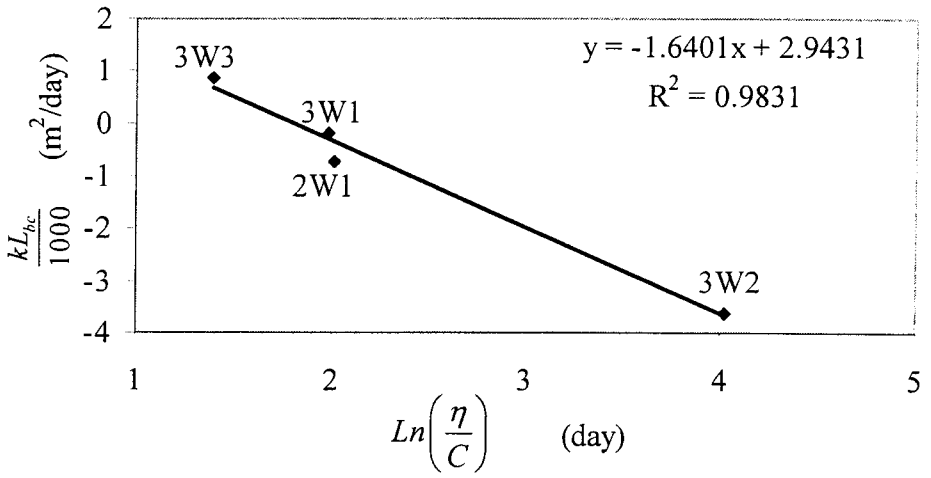

Figure 9. The linear relation of $Ln\left(\frac{\eta}{C}\right)$ and $\frac{kL_{bc}}{1000}$

CHAPTER 5. Conclusion

A one-dimensional visco-elastic model is developed to describe the groundwater level changes in the wells in the Cho-shui River alluvial fan after the Chi-Chi earthquakes. The model adequately reproduced the observed groundwater level changes after the earthquakes. The result supports our hypotheses that acceleration is important in the confined portion of the aquifers, while diffusion is the dominant process in the unconfined portion of the aquifers. Furthermore, we showed that the viscosity coefficient strongly correlates to the hydraulic conductivity of the aquifer. However, a general three-dimensional, heterogeneous model may be necessary to accurately describe groundwater changes in the fan.

Acknowledgements

This study was supported by the National Science Council of Taiwan under contract No. NSC 90-2625-Z-002-025. The authors are grateful to Water Resources Agency and Central Geological Survey of Taiwan for providing the field data.

References

Abamowitz, M., and I. A. Stegun, Handbook of mathematical functions with formulas, graphs, and mathematical tables, 1043 pp., Dover Publications, New York, 1972.

Biot, M. A., General theory of tree-dimensional consolidation, Journal of Applied Mechanics, 12, 155-164, 1941.

Biot, M. A., Theory of propagation of elastic waves in a fluid-saturated porous solid, I. low-frequency range, The Journal of the Acoustical Society of America, 28, 168-178, 1956a.

Biot, M. A., Theory of propagation of elastic waves in a fluid-saturated porous solid, II. high-frequency range, The Journal of the Acoustical Society of America, 28, 179-191, 1956b.

Central Geological Survey, The hydrogeological survey report of the Cho-Shui alluvial fan, Ministry of Economic Affairs, Taiwan, 1999. (in Chinese)

Central Geological Survey, The final survey report of the Cho-Shui alluvial fan, Ministry of Economic Affairs, Taiwan, 1994. (in Chinese)

Chia, Y. P., Y. S. Wang, H. P. Wu, C. J. Huang, C. W. Liu, M. L. Lin, and F. S. Jeng, Changes of ground water level in response to the Chi-Chi earthquake, in, Proceedings of International Workshop on Annual Commeration of Chi-Chi Earthquake, vol. I – Science Aspect, edited by Loh, C. H., and W. I. Liao, pp. 317-328, National Center for Reaearch on Earthquake Engineering, Taiwan, 2000.

Department of Land Administration, The records of the first and the second class GPS control stations, Ministry of the Interior, 2000. (digital records)

Farrell, O. J., and B. Ross, Solved problems: Gamma and Beta functions, Lendre polynomials, Bessel functions, 410 pp., Dover Publications, New York, 1971.

Flugge, W., Viscoelasticity, 194 pp., Springer-Verlag, New York, 1975.

Ge, S., and S. C. Stover, Hydrodynamic response to strike- and dip-slip faulting in half space, Journal of Geophysical Research, 105(B11), 25513-25524, 2000.

Green, and P. M. Naghdi, A dynamical theorem of interacting continua, International Journal of Engineering Science, 3, 241, 1965.

Hsieh, P. A., J. D. Bredehoeft, and J. M. Farr, Determination of aquifer transmissivity from earth-tide analysis, Water Resources Research, 78, 1824-1832, 1987.

Hsu, S. K., Plan for a groundwater monitoring network in Taiwan, Hydrogeology Research, 6, 405-415, 1998.

Huang, B. S., Two dimensional reconstruction of the surface ground motion of an earthquake: the September 21, 1999, Chi-Chi, Taiwan earthquake, Geophysical Research Letters, 27, 3025-3028, 2000.

Lin Y. P., C. C. Lee, and Y. C. Tan, Geostatistical approach for identification of transmissivity structure at Dulliu area in Taiwan, Environmental Geology, 40, 111-120, 2000.

Lin Y. P., Y. C. Tan, and S. Rouhani, Identifying spatial characteristics of transmissivity using simulated annealing and kriging methods, Environmental Geology, in press, 2001.

Ma, K. F., C. T. Lee, and Y. B. Tsai, The Chi-Chi, Taiwan earthquake: large surface displacement on an inland thrust fault, Eos (Transactions, American Geophysical Union), 80, 605-611, 1999.

O'Neil, P. V., Advanced engineering mathematics, 1456 pp., Wadworth Publishing Company, Belmont, California, 1991.

Water Conservancy Agency, Analysis for the changes of surface levels and ground water levels caused by the 921 Chi-Chi earthquake, Ministry of Economic Affairs, Taiwan, 2000. (in Chinese)

Water Conservancy Agency, The annual report of the Groundwater Monitoring Network System(GMNS) records in Taiwan, Ministry of Economic Affairs, Taiwan, 1999a. (in Chinese)

Water Conservancy Agency, The annual report of the daily flow records in Taiwan, Ministry of Economic Affairs, Taiwan, 1999b. (in Chinese)

Water Conservancy Agency, The annual report of the daily rainfall records in Taiwan, Ministry of Economic Affairs, Taiwan, 1999c. (in Chinese)

Yu, S. B., L. C. Kuo, Y. J. Hsu, H. H. Su, C. C. Liu, C. S. Hou, J. F. Lee, T. C. Lai, C. C. Liu, C. L. Liu, T. F. Tseng, C. S. Tsai, and T. C. Shin, Preseismic deformation and coseismic displacement associated with the Chi-Chi, Taiwan, earthquake, Seismological Society of America Bulletin, 2001. (in press).